

INTERACTION OF TITANIUM DIOXIDE NANOPARTICLE WITH HUMAN SERUM ALBUMIN: A SPECTROSCOPIC APPROACH

MOHD JAHIR KHAN AND MOHAMAD YUSOF MASKAT*

School of Chemical Sciences and Food Technology, Faculty of Science and Technology, Universiti Kebangsaan Malaysia, 43600 Bangi, Selangor Darul Ehsan, Malaysia. Email: maskatmy@yahoo.com

Received: 25 Nov 2013, Revised and Accepted: 18 Apr 2014

ABSTRACT

Objective: The present study is designed to investigate the interaction of titanium dioxide nanoparticle (TiO₂NPs) with human serum albumin (HSA) using spectroscopic techniques.

Methods: TiO₂NPs was characterized by transmission electron microscopy (TEM), dynamic light scattering (DLS) and Fourier transform infrared (FTIR) spectroscopy. Effect of NPs on the conformation of HSA was evaluated by UV-vis and fluorescence spectroscopies.

Results: The characterization result demonstrated that TiO₂NPs were somewhat spherical with average diameter of ~32 nm. UV-vis and fluorescence spectroscopic studies showed that NPs form ground state complex with HSA.

Conclusion: UV-vis and fluorescence spectroscopy depicted the formation of HSA-TiO₂NPs complex induced conformational changes in human serum albumin.

Keywords: Human serum albumin, Titanium dioxide nanoparticle, Protein-nanoparticle interaction, Protein conformation.

INTRODUCTION

Titanium dioxide nanoparticle (TiO₂NPs) is used extensively in paint, pigment, food, medicine and pharmaceuticals. More than 70% of the total produced TiO₂NPs is utilized as pigments owing to high brightness, large refractive index and resistance to discoloration [1, 2]. It reflects UV light more strongly than the natural bulk material of same composition thus, vastly applied in sunscreen and personal care products. In some products the amount of TiO₂NPs is even more than 10% by weight [3, 4].

Human being exposed to nanoparticle either accidentally such as occupational exposure or intentionally using nanoparticle enabled consumer products. The major routes of exposure are inhalation, oral/dermal contact and intravenous injection [5, 6]. It has been well documented that the nanoparticle, after entry into the bloodstream first interacts with biomolecules like proteins, lipids and nucleic acids.

Therefore, the effect of NPs is a combined effect of nanoparticle-protein "corona" rather than nanoparticle alone [7]. Adsorption of protein onto surface of nanoparticle may change its properties like orientation, conformation and packing arrangement. This may cause toxicity, diverse biological reactions and disease conditions [8-10]. Proteins undergo varying degree of conformational changes in the presence of NPs. Therefore, understanding of protein NPs interaction is a fruitful application of NPs in toxicology and medicine [11, 12].

HSA is the most abundant blood protein, plays key role in transport, distribution and metabolism of several exogenous and endogenous compounds such as drugs, metabolites, hormones, amino acids and fatty acids. It is a single polypeptide of 585 amino acid residues having 17 pairs of disulphide bridges and one free cysteine residue. Crystallographic studies of diverse HSA drug complexes demonstrated that the protein has two well-known ligand binding sites called sites I and site II, also called warfarin and benzodiazepine binding site, respectively. Site I is located within subdomain IIA while site II is present in subdomain III. The amino acids in these sites primarily determine the binding specificity of ligands. These domains have flexible structure so the conformation of protein may change after ligand binding. Apart from these numerous secondary binding sites are distributed across the protein [13, 14].

In the present study, we investigated the effect of TiO₂NPs on the conformation of HSA at physiological condition using spectroscopic techniques. The study is helpful in understanding the possible mechanism of interaction of TiO₂NPs with human serum albumin.

MATERIALS AND METHODS

HSA (fatty acid free) and TiO₂NPs were purchased from Sigma-Aldrich (St. Louis, MO, USA). All other chemicals and reagents were of analytical grade and used without any further purification.

Determination of protein concentration

All experiments were performed in 20 mM sodium phosphate buffer, pH 7.0 except where specified. The concentration of protein was determined with a double beam spectrophotometer (Shimadzu UV-2450 UV-vis Spectrophotometer) at 280 nm using specific absorption coefficient of 5.31 and alternatively by Lowry method [15].

Characterization of TiO₂NPs

A homogeneous suspension of TiO₂NPs was prepared by mixing dry powder in buffer at a concentration of 1 mg/mL. The suspension was sonicated for one hour using sonicator bath. A drop of NPs suspension was placed on carbon coated copper grid, air dried and then imaged with transmission electron microscope (JEOL, 2000FX, Japan) at an accelerating voltage of 200 KV. Dynamic light scattering (DLS) size measurement was carried out at 830 nm by DynaPro-TC-04 DLS equipment according to the procedure described by Khan et al [16]. Fourier transform infrared (FT-IR) spectrum was recorded with Perkin Elmer Spectrum BX, FT-IR (USA) at room temperature. Dry powder of NPs was dispersed into KBr matrix, mixed well and palletized. The pellet was kept in IR path and spectrum was measured in a range of 400-4000 cm⁻¹.

HSA-NPs interaction studies

HSA stock solution (5.0 mM) was prepared in 20 mM sodium phosphate buffer, pH 7.0 and diluted with the same buffer as per requirement. Protein concentration (25 μM) was kept constant throughout the study while NPs concentration varied from 0.2 to 2.0 mg/mL. The reaction mixture was first equilibrated at room temperature for 1hr and then UV-vis and fluorescence spectra were recorded to monitor the interaction of NPs with HSA.

UV-vis and fluorescence spectroscopy

The UV-vis absorption spectra were recorded with Shimadzu UV-VIS 2450 spectrometer (Shimadzu, Kyoto, Japan) equipped with 1.0 cm quartz cell. The spectra were taken in the wavelength range of 250-350 nm. For sample measurements, baseline was corrected with phosphate buffer, pH 7.0. Fluorescence analysis was performed with CARY-Eclipse spectrofluorometer (Varian, USA) equipped with a PC. Spectra were recorded at 37 ± 0.10 °C within the wavelength range of 300 to 450 nm, setting the excitation at 295 nm. The excitation and emission bandwidths were 5 and 10 nm, respectively. Each spectrum was scanned three times and finally average was used for plots and analyses.

RESULTS AND DISCUSSION

Characterization of NPs

The TEM image of TiO₂NPs is shown in Figure 1. It can be seen that the particle was slightly spherical with average diameter of ~32 nm. Some particles were larger in size because of the agglomeration/aggregation [17,18]. The size distribution of TiO₂NPs was further checked with dynamic light scattering (DLS) particle size analyzer and found that the average hydrodynamic diameter of NPs was ~42 nm (Fig. 2).

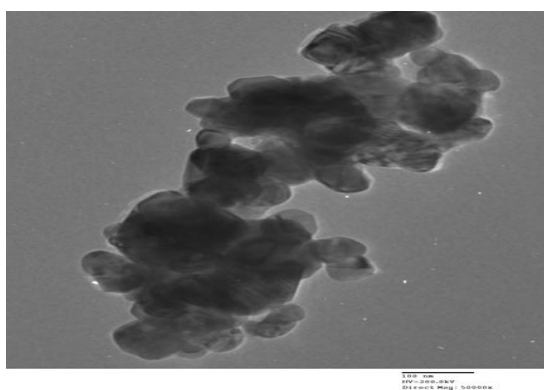


Fig. 1: Transmission electron micrograph of TiO₂NPs. The image was recorded with JEOL, 2000FX transmission electron microscope at an accelerating voltage of 200 KV.

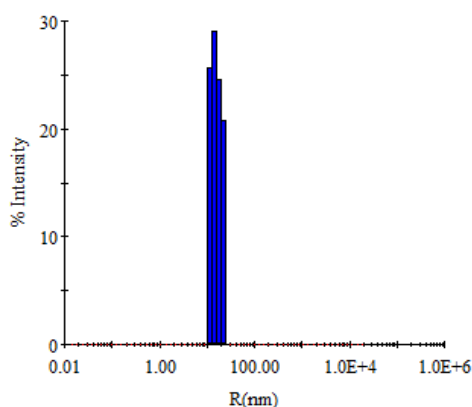


Fig. 2: The hydrodynamic size determination of TiO₂NPs by DynaPro-TC-04 DLS.

The bigger size of NPs in hydrodynamic state is because of the aggregation in aqueous medium [19,20]. Figure 3 shows FT-IR spectrum of TiO₂NPs. Absorption peaks at 3368 and 3770 cm⁻¹ were corresponded to O-H stretching mode of hydroxyl group, indicating the presence of moisture in the sample [21]. A strong peak at 1638 cm⁻¹ attributed to the stretching of titanium carboxylate. The

absorption bands below 1000 cm⁻¹ represents the oxide lattice vibrations of TiO₂ solid [22]. There was no C-H vibration band at 3000-2700 cm⁻¹ showed that the TiO₂NPs was free from organic compounds.

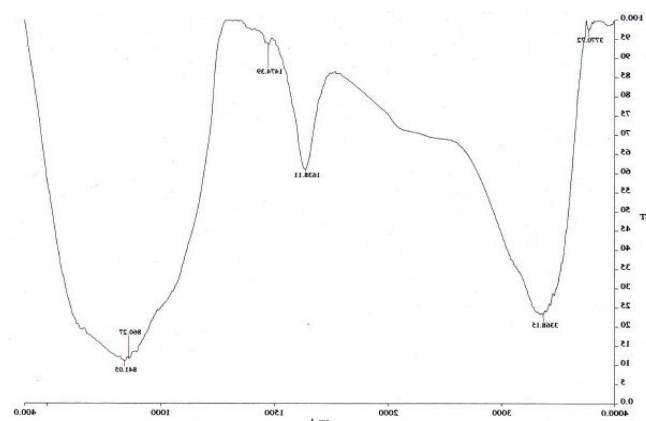


Fig. 3: FT-IR characterization of TiO₂NPs. Spectrum was recorded by Perkin Elmer, Spectrum BX, FT-IR instrument by KBr pellet method at room temperature.

UV-vis spectroscopy

UV-vis absorption spectroscopy is an effective and simple tool used to explore the structural changes in proteins [23]. The absorption spectra of HAS, Titrated with various amounts of TiO₂NPs is shown in Figure 4. A strong absorption peak of human serum albumin was observed at 280 nm due to the presence of aromatic amino acids for instance Phe, Tyr and Trp [24]. The absorption maxima of protein were decreased continuously with increasing concentration of NPs, indicating that some disturbance was occurred in the microenvironment of protein. This might be due to alteration of polypeptide chain which resulted in the conformational changes of protein [25].

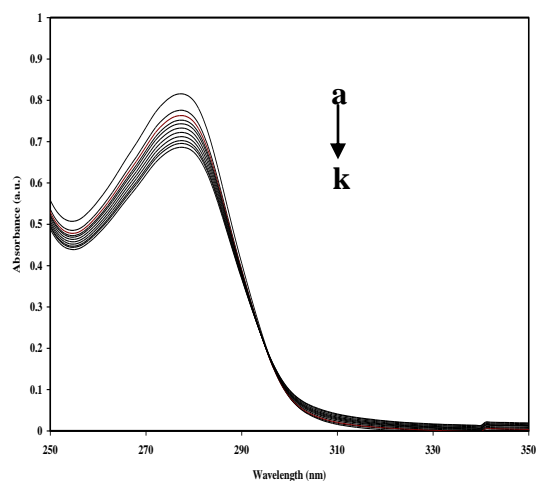


Fig. 4: UV-vis absorption spectra of HSA were recorded in the presence of varying amount of TiO₂NPs. The protein concentration was kept constant (25 μM) while NPs concentrations (a→k) varied as 0.0, 0.2, 0.4, 0.6, 0.8, 1.0, 1.2, 1.4, 1.6, 1.8 and 2.0 mg/mL.

Fluorescence Spectroscopy

Although, numerous techniques are available for protein ligand interaction studies but investigation of changes in the fluorescence intensity of protein due to quenching of ligand is a very important method [26, 27]. HSA has only one tryptophan residue present in the subdomain IIA [28]. The fluorescence intensity of HSA at 295 nm is

because of the tryptophan (Trp) moiety which is extremely sensitive to the local environment. Therefore, a trivial change in the microenvironment either by ligand binding or conformational transition would significantly quench it. The fluorescence quenching study of proteins in the presence NPs showed the relative accessibility of particle to the chromophore residue of protein [29]. The result showed that the fluorescence maximum intensity of protein decreased progressively with the increasing concentration of TiO₂NPs (Fig. 5). This indicates that the NPs strongly quench to the chromophore residue of protein. The possible quenching mechanism was determined by fitting the dependence of F_0/F on TiO₂NPs concentration based on a Stern-Volmer equation

$$F_0/F = 1 + K_{sv} [Q] = 1 + kq\tau_0 [Q]$$

where F_0 and F are the fluorescence intensities of proteins in the absence and presence of NPs, respectively, K_{sv} is the Stern-Volmer quenching constant, $[Q]$ is the molar concentration of TiO₂NPs, kq stands for bimolecular quenching constant and τ_0 is the average life time of HSA, is 10^{-8} s [30].

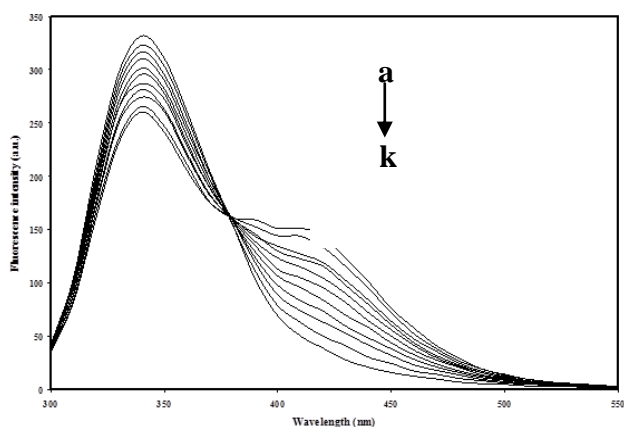


Fig. 5: Effect of TiO₂NPs on the fluorescence emission spectra of HSA. The concentration of protein was 25 μ M while NPs concentrations (a→k) varied as 0.0, 0.2, 0.4, 0.6, 0.8, 1.0, 1.2, 1.4, 1.6, 1.8 and 2.0 mg/mL.

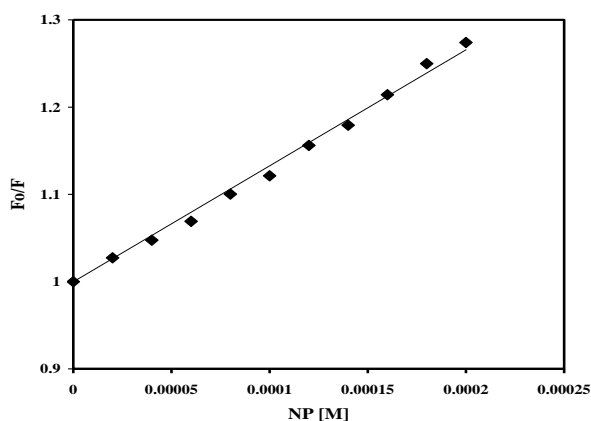


Fig. 6: Stern-Volmer plot for the binding of TiO₂NPs with HSA.

The result showed that plot of F_0/F versus $[Q]$ was linear and K_{sv} value derived at 37 °C was $1.3 \times 10^3 \text{ M}^{-1}$ (Fig. 6). Earlier studies showed that the binding of nanoparticles with HSA resulted in changes of fluorescence maxima of protein [31,32]. There are two main quenching mechanism includes dynamic and static. The former occurs when high energy quenchers collide with the excited-state fluorophores and brings it to the ground state while in static quenching a complex is formed between quenchers and ground-state fluorophores [33].

CONCLUSION

In the present study, the interaction of the HSA and TiO₂NPs was analyzed by UV-vis, and fluorescence spectroscopic techniques. Size of NPs was determined by DLS and TEM and found that the average size was ~ 32 nm. The conformation of HSA was changed in the presence of NPs as the UV-vis absorption as well as fluorescence spectra of protein were decreased with increasing concentrations of NPs. Furthermore, no spectral shift was observed in both the UV-vis absorption and fluorescence emission spectra revealed that NPs interacts to the protein away from Trp residue. The Stern-Volmer result indicated that the intrinsic fluorescence of HSA was quenched through static mechanism.

ACKNOWLEDGEMENT

The authors gratefully acknowledge to Universiti Kebangsaan Malaysia for the financial assistance.

REFERENCES

- Chen X, Mao S. Titanium dioxide nanomaterials: synthesis, properties, modifications, and applications. *Chem Rev* 2007;107: 2891-2959.
- Baan R, Straif K, Grosse Y, Secretan B, El Ghissassi F, Coglianò V. Carcinogenicity of carbon black, titanium dioxide, and talc. *Lancet Oncol* 2006;7: 295-296.
- Bengales MS, Mitkare SS, Gattani SG, Sakarkar DM. Recent nanotechnological aspects in cosmetics and dermatological preparations. *Int J Pharm Pharm Sci* 2012;4: 88-97.
- Brumfiel G. Consumer products leap aboard the nano bandwagon. *Nature* 2006;440: 262.
- Rajh T, Chen LX, Lukas K, Liu T, Thurnauer, MC, Tiede DM. Surface restructuring of nanoparticles: an efficient route for ligand-metal oxide crosstalk. *J Phys Chem B* 2002;106: 10543-10552.
- Zhu Y, Eaton JW, Li C. Titanium dioxide (TiO₂) nanoparticles preferentially induce cell death in transformed cells in a Bak/Bax-independent fashion. *PLoS ONE* 2012;7: e5060.
- Casals E, Pfaller T, Duschl A, Oostingh GJ, Puentes V. Time evolution of the nanoparticle protein corona. *ACS Nano* 2010;4: 3623-3632.
- Cedervall T, Lynch I, Lindman S, Berggård T, Thulin E, Nilsson H, Dawson KA, Linse S. Understanding the nanoparticle-protein corona using methods to quantify exchange rates and affinities of proteins for nanoparticles. *Proc Natl Acad Sci U S A* 2007;104: 2050-2055.
- Shultz MD, Ham YW, Lee SG, Davis DA, Brown C, Chmielewski J. Small-molecule dimerization inhibitors of wild-type and mutant HIV protease: A focused library approach. *J Am Chem Soc* 2004;126: 9886-9893.
- Longthorne VL, Williams GT. Caspase activity is required for commitment to fas-mediated apoptosis. *EMBO J* 1997;16: 3805-3817.
- Laera S, Ceccone G, Rossi F, Gilliland D, Hussain R, Siligardi G, Calzolari L. Measuring protein structure and stability of protein-nanoparticle systems with synchrotron radiation circular dichroism. *Nano Lett* 2011;11: 4480-4484.
- Shang W, Nuffer JH, Dordick JS, Siegel RW. Unfolding of ribonuclease A on silica nanoparticle surfaces. *Nano Lett* 2007;7: 1991-1995.
- He XM, Carter DC. Atomic structure and chemistry of human serum albumin. *Nature* 1992;358: 209-215.
- Ascenzi P, Fasano M. Allosterism in a monomeric protein: the case of human serum heme-albumin. *Biophys Chem* 2010;148: 16-22.
- Lowry OH, Rosenbrough NJ, Farr AL, Randall RJ. Protein measurements with the folin phenol reagent. *J Biol Chem* 1951;193: 265-275.
- Khan MJ, Husain Q, Ansari SA. Polyaniline-assisted silver nanoparticles: a novel support for the immobilization of α -amylase. *Appl Microbiol Biotechnol* 2013;97: 1513-1522.
- Jiang JK, Oberdorster G, Biswas P. Characterization of size, surface charge, and agglomeration state of nanoparticle dispersions for toxicological studies. *J Nanopart Res* 2009;11: 77-89.

18. Wang BQ, Jing LQ, Qu YC, Li SD, Jiang BJ, Yang LB, Xin BF, Fu HG. Enhancement of the photocatalytic activity of TiO₂ nanoparticles by surface-capping DBS groups. *Appl Surface Sci* 2006;252: 2817-2825.
19. Hussain S, Thomassen LC, Ferecatu I, Borot MC, Andreau K, Martens JA, Fleury J, Baeza-Squiban A, Marano F, Boland S. Carbon black and titanium dioxide nanoparticles elicit distinct apoptotic pathways in bronchial epithelial cells. *Part Fibre Toxicol* 2010;7: 10.
20. Patri A, Umbreit T, Zheng J, Nagashima K, Goering P, Francke-Carroll S, Gordon E, Weaver J, Miller T, Sadrieh N, McNeil S, Stratmeyer M. Energy dispersive X-ray analysis of titanium dioxide nanoparticle distribution after intravenous and subcutaneous injection in mice. *J Appl Toxicol* 2009;29: 662-672.
21. Soler-Illia G, Louis A, Sanchez C. Synthesis and characterization of mesostructured titania-based materials through evaporation-induced self-assembly. *Chem Mat* 2002;14: 750-759.
22. Grassian VH, O'shaughnessy PT, Adamcakova-Dodd A, Pettibone JM, Thorne PS. Inhalation exposure study of titanium dioxide nanoparticles with a primary particle size of 2 to 5 nm. *Environ Health Perspect* 2007;115: 397-402.
23. Wang J, Wang Y, Gao J, Hu P, Guan H, Zhang L, Xu R, Chen X, Zhang X. Investigation on damage of BSA molecules under irradiation of low frequency ultrasound in the presence of FeIII-tartrate complexes. *Ultrason Sonochem* 2009;16: 41-49.
24. Naveenraj S, Anandan S, Kathiravan A, Renganathan R, Ashokkumar M. The interaction of sonochemically synthesized gold nanoparticles with serum albumins. *J Pharm Biomed Anal* 2010;53: 804-810.
25. Glazer AN, Smith EL. Studies on the ultraviolet difference spectra of proteins and polypeptides. *J Biol Chem* 1961;236: 2942-2947.
26. Chadborn N, Bryant, J, Bain AJ, O'Shea P. Ligand-dependent conformational equilibria of serum albumin revealed by tryptophan fluorescence quenching. *Biophys J* 1999;76: 2198-2207.
27. Gao D, Tian Y, Bi S, Chen Y, Yu A, Zhang H. Studies on the interaction of colloidal gold and serum albumins by spectral methods. *Spectrochim Acta A Mol Biomol Spectrosc* 2005;62:1203-1208.
28. Jones RR, Harkrader RJ, Southard GL. The effect of pH on sanguinarine iminium ion form. *J Nat Prod* 1986;49: 1109-1111.
29. Lakowicz JR, Weber G. Quenching of fluorescence by oxygen. A probe for structural fluctuations in macromolecules. *Biochemistry* 1973;12: 4161-4170.
30. Togashi DM, Ryder AG. A fluorescence analysis of ANS bound to bovine serum albumin: binding properties revisited by using energy transfer. *J Fluoresc* 2008; 18: 519-526.
31. Hemmateenejad B, Yousefinejad S. Interaction study of human serum albumin and ZnS nanoparticles using fluorescence spectrometry. *J Mol Struct* 2013;1037: 317-322.
32. Sen T, Mandal S, Haldar S, Chattopadhyay K, Patra A. Interaction of gold nanoparticle with human serum albumin (HSA) protein using surface energy transfer. *J Phys Chem C* 2011;115:24037-24044.
33. Hu, YJ, Liu Y, Zhao RM, Dong JX, Qu SS. Spectroscopic studies on the interaction between methylene blue and bovine serum albumin. *J Photochem Photobiol A* 2006;179: 324-329.